Laser Micromachining of Barium Titanate ($BaTiO_3$)-Polymer Nanocomposite Based Flexible/Rollable Capacitors

Rabindra N. Das, Frank D. Egitto, John M. Lauffer, and Voya R. Markovich
Endicott Interconnect Technologies, Inc.
1093 Clark Street, Endicott, New York, 13760.
Telephone No: 607-755-1389
E-mail: rabindra.das@eitny.com

Abstract
This paper discusses laser micromachining of thin films. In particular, recent developments on high capacitance, large area, thin, flexible/rollable embedded capacitors are highlighted. A variety of flexible nanocomposite thin films ranging from 2 microns to 25 microns thick were processed on copper or organic substrates by large area (330 mm × 470 mm, or 495 mm X 607 mm) liquid coating processes. SEM micrographs showed uniform particle distribution in the coatings. Nanocomposites resulted in high capacitance density (10-100 nF/inch^2) and low loss (0.02-0.04) at 1 MHz. The remarkably increased flexibility of the nanocomposite is due to uniform mixing of nanoparticles in the polymer matrix, resulting in an improved polymer-ceramic interface. $BaTiO_3$-epoxy polymer nanocomposites modified with nanomaterials were also fabricated and were investigated with SEM analysis. Capacitance density of nanomaterial-modified films was increased up to 500 nF/inch^2, about 5-10 times higher than $BaTiO_3$-epoxy nanocomposites. A frequency-tripled Nd:YAG laser operating at a wavelength of 355 nm was used for the micromachining study. The micromachining was used to generate arrays of variable-thickness capacitors from the nanocomposites. The resultant thickness of the capacitors depends on the number of laser pulses applied. Laser micromachining was also used to make discrete capacitors from a capacitance layer. In the case of sol-gel thin films, micromachining results in various surface morphologies. It can make a sharp step, cavity-based wavy structure, or can make individual capacitors by complete ablation. Altogether, this is a new direction for development of multifunctional embedded capacitors.

Introduction

Organic/Polymer/Nanocomposite materials have attracted a lot of attention for building large-area, mechanically flexible electronic devices [1-6]. Organic light-emitting diodes for flat-panel displays appear ready for mass production [7,8], and significant progress has also been made in organic thin-film transistors [9], and solar cells [10,11]. There is also a strong desire to develop new large scale advanced materials that can meet the growing demand for miniaturization, high-speed performance, and flexibility for microelectronic products. An effort in this direction is presented in this paper.

Passives account for a very large part of today's electronic assemblies. This is particularly true for digital products such as cellular phones, camcorders, and computers. Market pressures for new products with more features, smaller size and lower cost drive the demand for smaller, compact, complex circuit boards. An obvious strategy is to reduce the number of surface mounted passives by embedding them in the substrate or printed wire boards. In addition, current interconnect technology to accommodate surface mounted passives impose certain limits on board design, which limit the overall circuit speed. Embedding passives are one way to save substrate real estate, conversion cost, reduce parasitic effects and improve performance [12].

Among the various passives, embedded capacitors deserve special attention as they provide the greatest potential benefit for high density, high speed, and low voltage IC packaging. Capacitors can be embedded into the interconnect substrates (printed wiring board, flex, MCM-L, interposer) to provide decoupling, bypass, termination, and frequency determining functions [13,14]. Available commercial polymer composite technology is not adequate for high capacitance density, thin film embedded passives. Several polymer nanocomposite studies so far have been focused on processing of high capacitance density thin films within small substrates/wafers [15-19]. One of the important processing issues in thin film polymer nanocomposite-based capacitors is to achieve high capacitance density on large coatings. This high capacitance/dielectric constant on large coatings is also important to commercialize low operating voltage organic transistors for RFID and display applications [20-22]. Recent interest in the development of flexible electronics such as roll-up displays, e-papers, and keyboards reinforces the need for flexible embedded components such as embedded capacitors.

Barium titanates, $BaTiO_3$ have become increasingly important in the electronics industry, because of their ferroelectric, piezoelectric and thermoelectric properties. Recent advances in nanotechnology, which spans the synthesis of nanoscale meter, understanding/utilizing their exotic electronic properties, and organization of nanoscale structures into predefined superstructures, promises to play an increasingly important role in many key technologies[23-29]. In this paper, we report novel barium titanate ($BaTiO_3$)-polymer based nanocomposites that have the potential to surpass conventional composites to produce thin film capacitors over large surface areas, having high capacitance density and low loss. Specifically, the focus is on new flexible composite dielectric materials that can be integrated into boards, laminate chip carriers (LCCs), or roll-to-roll manufacturing processes. A variety of nanocrystalline $BaTiO_3$ powders were utilized with the objective of manufacturing low-cost, high-performance, flexible nanocomposites with subsequent laser micromachining of the nanocomposites to produce novel micromachined 3D capacitors. Micromachining technologies can produce variable thickness and discrete capacitors from a single sheet (layer) of capacitors. Both types of capacitors can be integrated in the same layer (**Figure 1**). Moreover, an improved micromachining technique was developed to control the surface morphology of sol-gel thin films. Experimental data shows micromachining is highly efficient for controlling film thickness. With this method, new structures can be designed without altering the dielectric properties of the nanocomposites. The technique can be used to generate multi-functional capacitors.

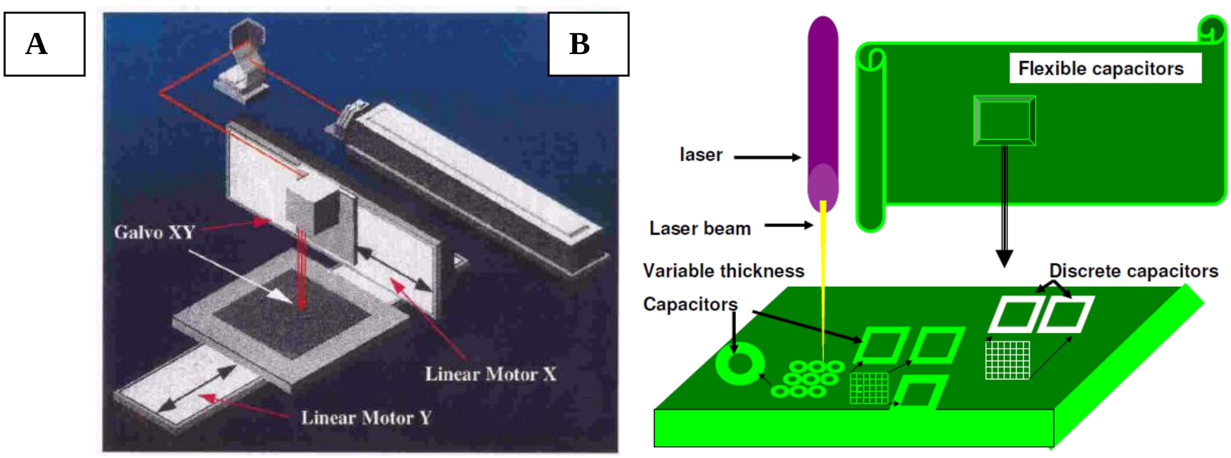

Figure 1: Schematic representations (A) laser processing (source: ESI, Inc.), and (B) micromachining: top views showing arrays of discrete and variable-thickness capacitors.

2. Experimental Procedure

A variety of $BaTiO_3$ nanoparticles and their dispersion into epoxy resin were investigated in order to achieve a thin uniform film. In a typical procedure, $BaTiO_3$-epoxy nanocomposites were prepared by mixing appropriate amounts of the $BaTiO_3$ nano powders and epoxy resin in organic solvents. A thin film of this nanocomposite was then deposited on a copper substrate and cured. Barium titanate ($BaTiO_3$)-epoxy polymer nanocomposites modified with nanomaterials were also prepared. In the case of laminates, two thin films were prepared, dried, and then laminated together. $BaTiO_3$-sol-gel thin films were prepared from a 0.5 molar aqueous acetate solution of Ba $(CH_3COO)_2$ and Ti $(OC_2H_5)_4$. The film was deposited on Si or glass substrates by spin coating, and dried successively at 150° and 450°C to remove all the organics. The film was then annealed at ~600°C in air to generate a crystalline phase.

Figure2: Larger area SEM image of composite specimens: (A) $BaTiO_3$-epoxy (B) $BaTiO_3$-fluoropolymer nanocomposites.

Laser micromachining was performed on an ESI (Electro Scientific Industries, Inc., Portland, OR) 5210 Laser Microvia Drill System. A frequency-tripled Nd:YAG laser operating at a wavelength of 355 nm was used. The pulse width of the laser was on the order of 50 ns. The beam was positioned relative to the surface of the work piece by coordinated motion of the stage on which the sample is mounted (y-axis), the optics (x-axis), and galvo mirrors (x and y axes). The position of the sample with respect to the focal plane of the imaged laser beam (along the z-axis) can also be adjusted. The spatial distribution of energy in the circular laser spot is homogenized by use of ESI-supplied optics. In this instance, beam diameter at the surface of the workpiece was varied by adjusting the relative position of the imaged beam with respect to the surface of the film. Other salient parameters are listed in the table below. Parameters are defined as follows.

Rep Rate is the number of laser pulses delivered to the workpiece per unit time.
Power is the average power of the laser.
Z-Offset is the relative position of the imaged beam with respect to surface of the substrate; a negative number indicates that the beam is imaged below the surface.
Velocity is the speed at which the beam is traced along the programmed beam path.
Repetitions is the number of times the system traces the programmed beam path.
Bite Size is the distance the system moves the beam relative to the workpiece between pulses, along the programmed beam path.

Direct laser ablation of nanocrystalline $BaTiO_3$ filled epoxy was performed using the parameters given in the table below. The $BaTiO_3$ filled epoxy nanocomposite film was micromachined using a variety of conditions to form various surface morphologies and capacitors arrays.

Material Thickness (um)	2.5	8.5
Power (watts)	0.3	0.3
Z-Offset (mm)	-0.45	-0.45
Rep Rate (kHz)	12	12
Repetitions	4	13
Bite Size (um)	8.33	8.33
Velocity (mm/sec)	100	100

Electrical properties (capacitance, Dk, loss) of the nanocomposite thin films were measured at room temperature using an impedance/gain-phase analyzer (Model 4194A, HEWLETT-PACKARD). Surface morphology and particle distributions of nanocomposite films were characterized by a LEO 1550 scanning electron microscope (SEM). Micromachining depths of films were determined by optical microscope and SEM.

Figure 3: Photographs of flexible capacitance layers.

3. Results and Discussion

A real challenge in the development of large area thin film nanocomposites is the incompatibility that exists between the typically hydrophilic nanoparticles and hydrophobic polymer matrix, which leads to nanoparticle agglomeration. As a result inferior coatings with poor performance are obtained. We have identified proper surface treatment that results in excellent dispersability[5,25] of the nanoparticles and good quality, monolithic coatings. Surface treatment of ceramics depends on its processing routes. Ramesh et al[19] reported silane treatment of hydrothermally prepared $BaTiO_3$ nanoparticles. The finer details of the particles and their surface morphologies were investigated using SEM. **Figure 2** show scanning electron micrographs of nanocomposite thin films. Nanoparticles formed uniform dispersion in the epoxy/fluoropolymer matrix. The particles in the epoxy matrix are so intimately compacted that analysis of individual particles is difficult. However, closer observation of the micrographs clearly reveals a uniform distribution of closely packed, well connected particles. Figure **2(A)** and **2(B)** show surface morphologies of nanocomposites consisting of 120 nm particles.

Figure 3 shows two large-area, flexible, thin film sheets of capacitor material. Capacitors can be bent or rolled without damaging the structure. For conventional composites, rolling or bending will cause structural damage such as cracking. The remarkably increased flexibility of the nanocomposite is due to uniform mixing of nanoparticles in the polymer matrix, resulting in an improved polymer-ceramic interface. Integration of this flexible capacitance layer into a flexible structure could be useful for developing high performance multilayer flexible electronics, such as roll-up displays, e-papers, and keyboards.

The electrical properties of ~2-100 mm^2 capacitors fabricated from nanocomposite thin films showed high capacitance density ranging from 10 nF/$inch^2$ to 100 nF/$inch^2$, depending on composition, particle size, and thickness of the coatings. Thin film capacitors fabricated from 40-60% v/v $BaTiO_3$ epoxy nanocomposites showed a capacitance density in the range of 40-80nF/$Inch^2$ that was stable over a frequency range of 1MHz to 10 MHz. Electrical properties of capacitors fabricated from ~70% v/v nanocomposite showed capacitance density of about 100nF/$inch^2$. For a particular composition, both capacitance density and dielectric loss increase with decreasing thickness**. Figure 4** shows the room temperature capacitance profile measured at 1MHz - 10 MHz for a $BaTiO_3$ epoxy nanocomposite thin film as a typical representative example. It was found that with increasing frequency (1-10 MHz), the capacitance density decreased. Change in capacitance with frequency was less pronounced in the case of thicker films. All nanocomposites below 60 vol% passed 100 volt test, which is high enough for the nanocomposite to serve as an insulating material embedded capacitor. Similarly, tensile strength with 1 oz copper for all nanocomposites below 60 vol% was found to be higher than 3700 PSI. Ramesh et al[19] reported over 200 nF/$inch^2$ capacitance density from a submicron surface-modified nanocomposite film obtained from spin coating process. The current material set can also produce high capacitance from a submicron-thick spin-coated film deposited on a small copper substrate. However, film quality degrades when deposited on a large substrate. Capacitance density of nanomaterial-modified films was 500 nF/$inch^2$, about 5-10 times higher than obtained with $BaTiO_3$-epoxy nanocomposites.

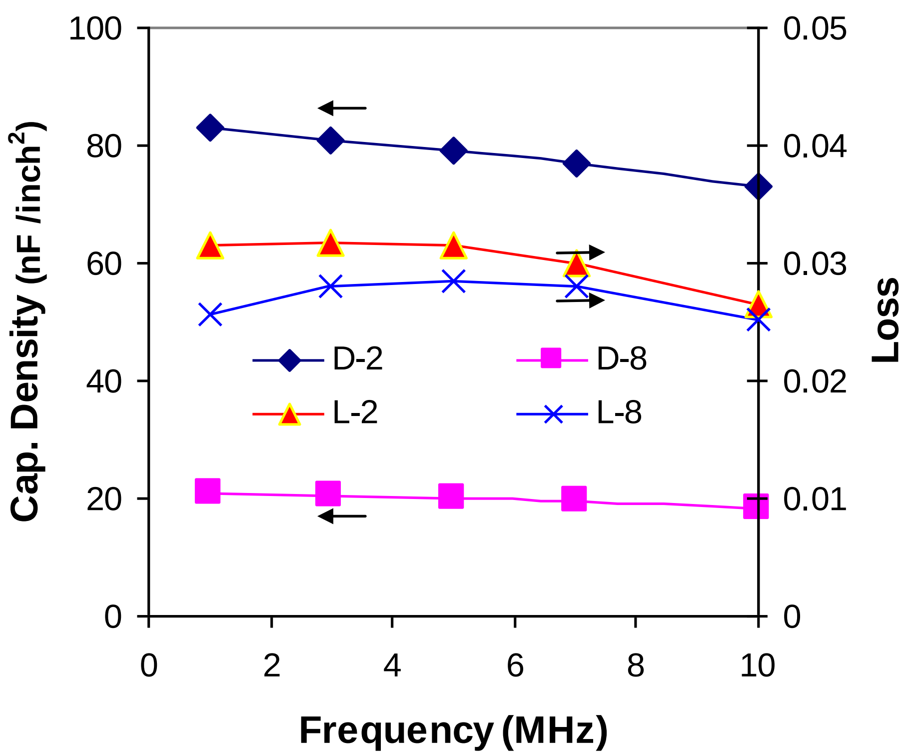

Figure 4: Capacitance density and loss as a function of frequency and thickness. D-8 and L-8 represent capacitance density and loss, respectively, of 8.5 microns thin film. Similarly, D-2 and L-2 represent capacitance density and loss of 2 microns thin film.

Figure 5A shows a top view of laser micromachined capacitor arrays. The basic structure consists of two layers: the micromachined capacitor and the substrate. Using this method, fully micromachined capacitors can be consistently generated. SEM micrographs are shown in Figures 5B to 5D for a series of arrays machined using varying numbers of laser pulses. The depth of microfabricated capacitors varies from 4 microns to 70 microns, depending on the number of laser pulses. The surface smoothness of the ablated areas that define the laser micromachined capacitors depends upon the uniformity of the spatial energy distribution of the laser beam. Although the smoothness of the ablated regions shown in Figure5 is not optimum, adjustment of the optics used in the present study could produce a more homogeneous energy profile for the beam. Alternatively, excimer laser micromachining systems have been shown to produce very uniform ablation over reasonably large areas.

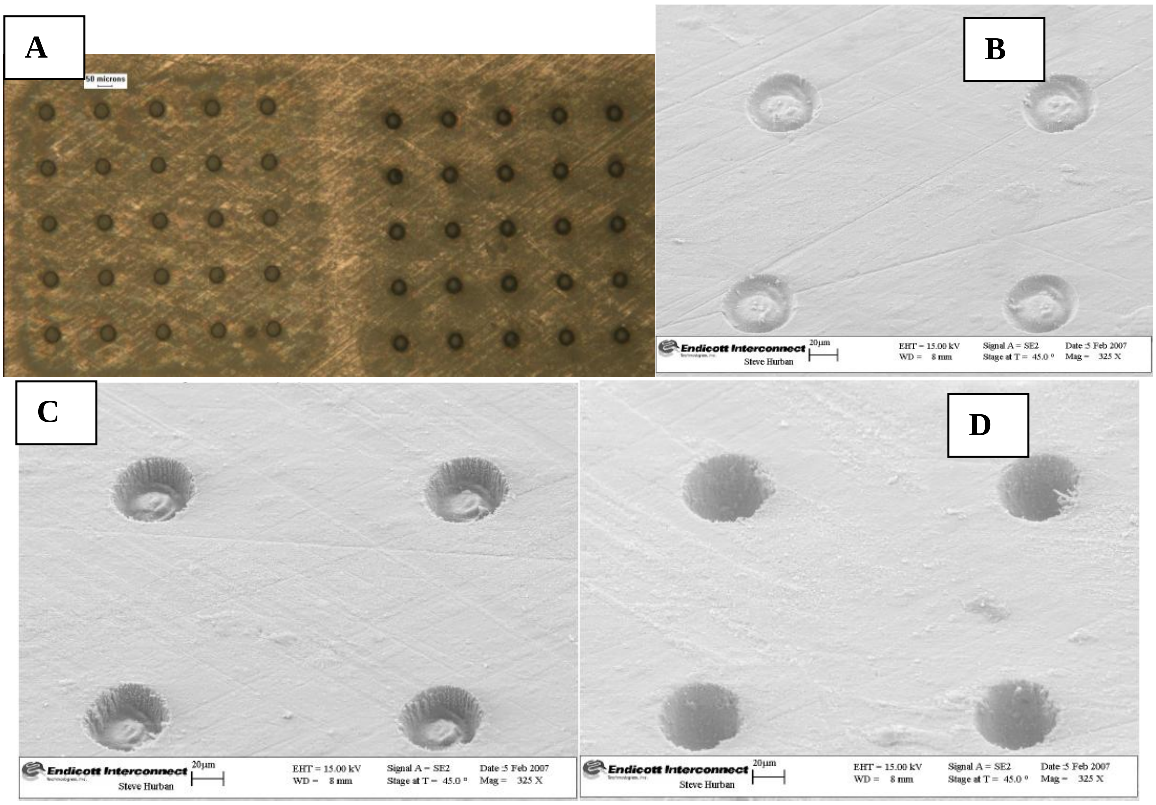

Figure 5: Micromachined nanocomposite-based capacitor array (A) Optical photograph, (B) SEM micrograph of array machined with 20 pulses, (C) micrograph of array machined with 50 pulses, and (D) micrograph of array machined with 200 pulses.

Figure **6 (A, B)** shows variation of the depth of the micromachined areas with the number of laser pulses. Figure 6B also shows possible capacitance density (nF/inch2) for a 15 micron capacitor film assuming a dielectric constant 30. The thickness of the capacitors decreases with an increasing number of laser pulses. It is clear from Figure 6 (A, B) that as the depth of the micromachined area is increased (thickness of the remaining dielectric reduced), the corresponding capacitance increases. In other words, micromachining can generate capacitor libraries (arrays) with variable capacitance density. Increasing the number of pulses eventually results in complete removal of the dielectric. This would be useful for making discrete capacitors from a capacitance layer. Figure 7 shows a representative example of discrete capacitors formed from a larger capacitance layer. Figure 7B represents a 3D optical micrograph where the capacitor dielectric was removed to the point where the bottom electrode was exposed.

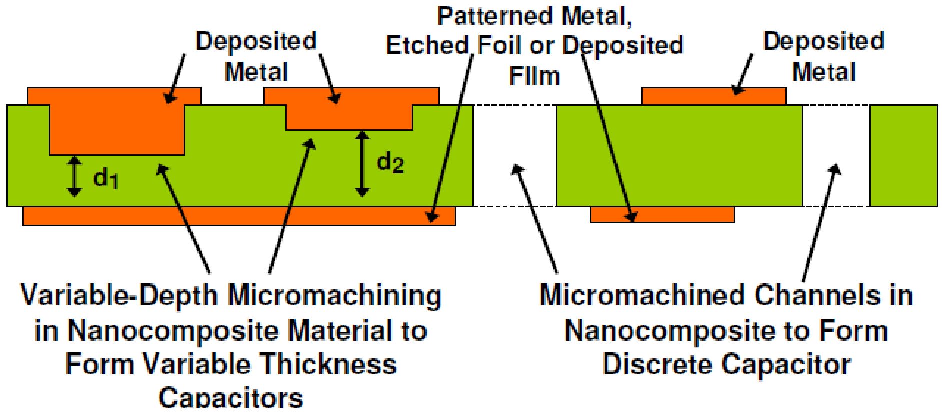

Figure 6A: Schematic cross-sectional views showing arrays of discrete and variable-thickness capacitors.

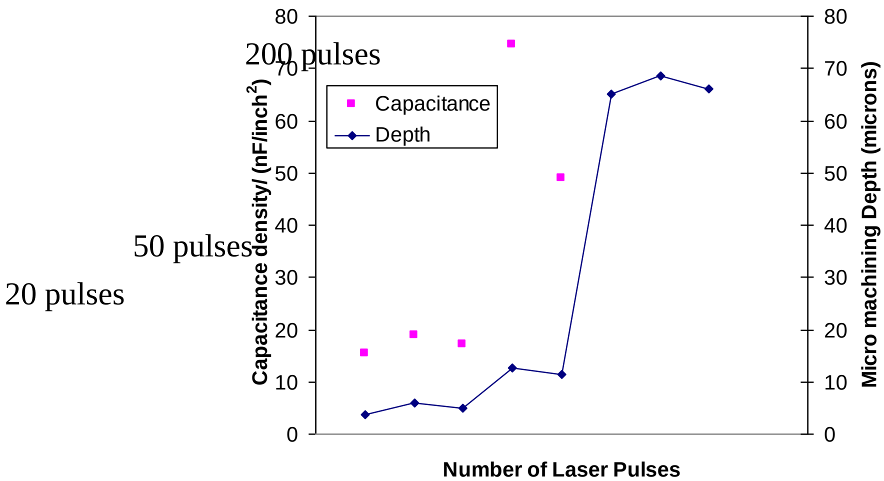

Figure 6B: Variation of depth with the number of laser pulses for a $BaTiO_3$ nanocomposite (Dk =30). Theoretical calculation of capacitance change with number of laser pulses for nanocomposite thin film (Dk =30, thickness = 15 micron).

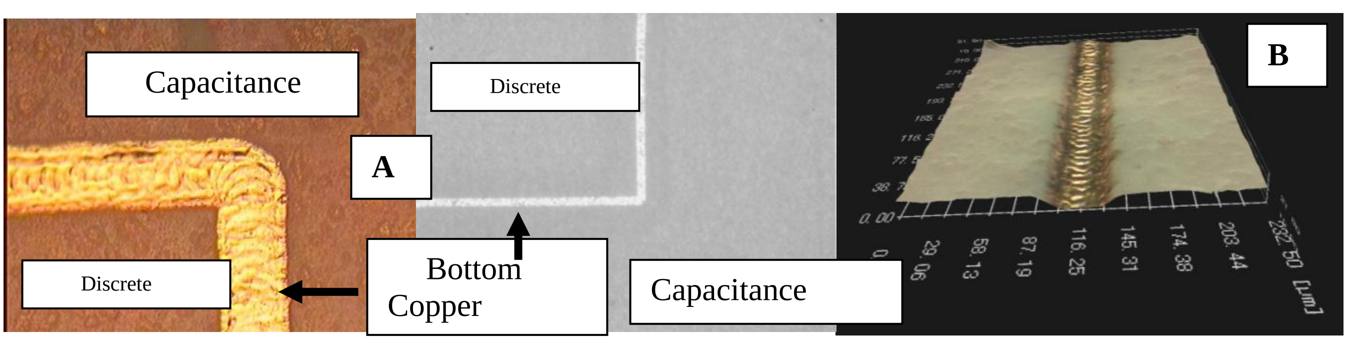

Figure 7: Laser micromachining produces discrete capacitor from a capacitance layer (A) Optical photograph (B) Optical 3D photograph of another sample.

For $BaTiO_3$/PZT based sol-gel thin films exposed to high energy density, material absorption favors ablation. On the other hand, when sol-gel thin films are exposed to the same laser at low energy density, material absorption favors annealing.

The surface topography of the $BaTiO_3$ thin film surfaces was examined by performing SEM, and optical imaging. **Figure 8** shows different surface morphologies generated by variation of laser fluence. Sufficiently strong laser pulses induce local melting and rapid cooling, leading to formation of an amorphous particle. One can use laser irradiation to raise the temperature of the film above the crystallization temperature, but below the melting temperature, thus converting an amorphous region to a crystalline phase. **Figures 8A and 8B** represent typical examples of melting and solidification of amorphous particles. Ablation was observed at very high energy densities. With a gradual decrease in energy, but still at high enough fluence values, the central part of the area traced by the laser beam path completely melts, whereas the adjacent surrounding area appears to be partially melted.

Laser processing of the as-deposited $BaTiO_3$ film leads to a noticeable conversion from a smooth surface to wavy cavity structure as can be seen in the SEM and optical images (**Figures. 8C, D, and E**). This is apparently due to local melting of the top surface induced by the transient laser heating. Similar melting behavior has been observed in pulsed laser deposition of ZnO films upon laser annealing at 193 nm. The annealing substantially reduces the surface grain structure and generates a new porous channel-like network reminiscent of a labyrinth structure. Each channel has an average width of about 2 to 5 microns and depth of about 0.1 to 0.5 micron. It is interesting to note that all the laser-annealed/micromachined spots, irrespective of their location on the film (center or periphery), maintain almost the same kind of channel structure. Moreover, it can be created in selective locations. This kind of structure was shown to be critical for achieving laser-like action upon optical pumping as it favors efficient coupling of the pump light into the film material[31] . Excess laser energy favors ablation. It can be seen that at high laser energy, the barium titanate film is ablated and the underlying silicon surface exposed (**Figure 8F**).

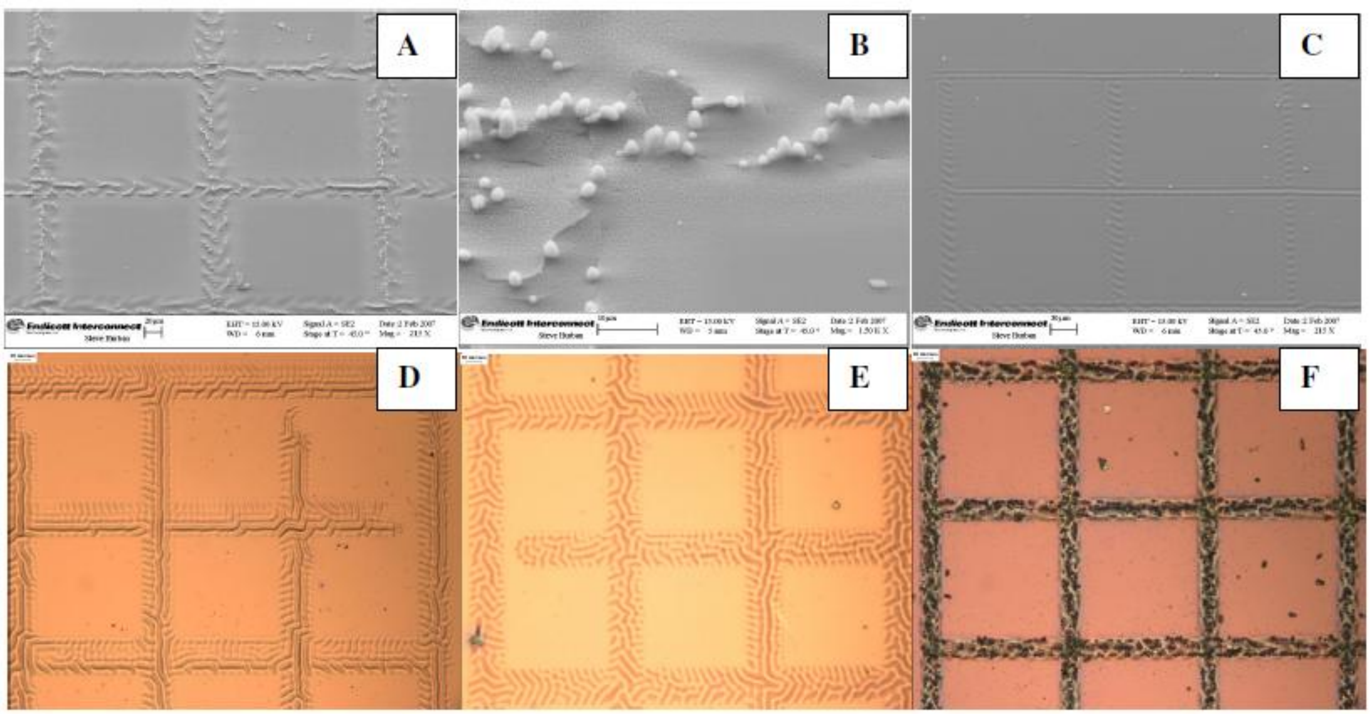

Figure 8: SEM micrographs and optical photographs of laser micromachined sol-gel thin films; (A) and (B) Low and high magnification SEM micrographs of thin films with surface particles, (C) to (E) SEM micrograph and optical photographs of thin films with a wavy, channel-like structure, and (F) Optical photograph of a micromachined (ablated) thin film surface for which the sol-gel thin film has been completely removed in the channels..

4. Conclusions

A thin film technology based on $BaTiO_3$-epoxy polymer nanocomposites was developed to manufacture high-performance, large-area, flexible/rollable, thin film capacitors. It is possible to produce very thin films, on the order of 2 microns, using the nanocomposites. The remarkable flexibility and thickness of the nanocomposite is due to uniform mixing of nanoparticles in the polymer matrix which results in improved polymer-ceramic interfaces. A frequency-tripled Nd:YAG laser operating at a wavelength of 355 nm was used for the micromachining study. We have shown a variety of micromachined surfaces suitable for multifunctional capacitor applications. Lasers can provide various complex micromachined patterns. This technique can be used to prepare capacitors of various thicknesses from the same capacitance layer, and ultimately can produce variable capacitance density, or a library of capacitors. The process is also capable of making discrete capacitors from a single layer of capacitance material. As the demand grows for complex multifunctional embedded components for advanced organic packaging, laser micromachining will continue to provide unique opportunities.

References

1. Friend R. H., Gymer R. W., Holmes A. B., Burroughes J. H., Marks R. N., Taliani C. , D. D. C., Bradley D.Dos Santos A., Brédas J. L., Lögdlund M, Salaneck M. R., *Nature* **1999**, 397, 121
2. Dimitrakopoulos C.D., Malentant P. R. L., *Adv. Mater*.2002,14,99
3. Alam MA, Pimparkar N, Kumar S, Murthy J, *MRS Bulletin* 2006,31,466
4. Z. Bao, Rogers JA and Kartz HE, *J. Mater. Chem.* 1999,9, 1895
5. Anglos D , Stassinopoulos A, Das RN, Zacharakis G, Psyllaki M, Anastasiadis S.H, Vaia R.A, Giannelis E.P. (feature issue), *J. Opt. Soc. Amer B*, 2004,21, 208.
6. Lappas A, Zorko A, Wortham E, Das RN, Giannelis EP, Cevc P, and Arcon D, *Chem. Mater.*,2005,17,1199
7. Howard W. E., *Sci. Am*. 2004, 290, 76.
8. Sirringhuas H., Tessler N., Friend R. H., *Science* 1998, 280, 1741.
9. Dimitrakopoulos C. D., Mascaro D. J., *IBM J. Res. Dev*. 2001, 45,11.
10. Yu G., Gao J. , Hummelen J. C., Wudl F., Heeger A. J., *Science* 1995, 270, 1789.
11. Brabec C. J., Sariciftci N. S., Hummelen J. C., *Adv. Funct. Mater.* 2001, 11, 15.
12. Jillek W. and Yung W. K. C., *International Journal of Advanced Manufacturing Technology* 2005,25, 350.
13. “Passive Integration: Easier Said Than Done”, *Prismark Partners LLC*, August 1997
14. Post J. E., “*Microwave and Optical Technology Letters* 2005, 46, 487.
15. Devaraju N.G., Kim ES, Lee BI, *Microelectronic Engineering*,2005, 82,71
16. Rao Y., Ogitani S., Kohl P., Wong C. P., *Journal of Applied Polymer Science* 2002, 83, 1084.
17. Rao Y., Wong C. P., *Journal of Applied Polymer Science* 2004, 92, 2228.
18. Windlass H., Raj P. M., Balaraman D., Bhattacharya S. K., and Tummala R. R., *IMAPS International Symposium on Advanced Packaging Materials*, Braselton, 2001, pp. 393-398
19. Ramesh S., Shutzberg B. A., Haung C., Gao J., Giannelis E. P., *IEEE Transactions on Advanced Packaging* 2003, 26, 17.
20. Dimitrakopoulos C., Mascaro D., *IBM Journal of Research and Development* 2001,45, 11
21. Edzer H., Huitema A., Gelnick G., Bas J., Putten P. V. D., Kuijk K., | Hart K.,| Cantatore K., and Leeuw D. de, *Adv. Mater*2002,14,1201
22. Ma L. and Yang Y., *Appl. Phys. Lett.* 2004,85, 5084
23. O'Brien S, Brus L, Murray CB, *J. Amer. Chem. Soc.*2003,123, 12085
24. Yun WS, JJ Urban, Q. Gu , *Nano Letters* 2002,2,447
25. Das RN, Law C, Zergioti I, Thompson M, Giannelis EP, “Combinatorial laser processing of ferroelectric thin and thick films” *Materials Research Society Symposium Proceedings*, Vol. Vol. 748, U12.18.1 (2003).
26. Mao YB, Banerjee S, Wong SS, *J. Amer. Chem. Soc.*2003,125,15718
27. Niederberger M, Garnweitner G, Pinna N, Antonietti M , *J. Amer. Chem. Soc.* 2004,126, 9120
28. Das RN and Pramanik P, *Nanotechnology*, 2004,15, 279
29. Spanier JE, Kolpak AM, Urban JJ, Grinberg I, Lian OY, Yun WS, Rappe AM, Park H, *Nano Letters* 2006, 6, 735
30. Das R. N., Pramanik P., "Low temperature chemical synthesis of Nano size ceramics" *British Ceramic Transactions* 2000, 99, 153.
31. A. Stassinopoulos, R. N. Das, E. P. Giannelis, S. H. Anastasiadis, D. Anglos “Random lasing from surface modified ZnO films of ZnO nanoparticles” Applied Surface Science,2005,247,18-24